



52 The major drawback of conventional homogeneous (gas-phase) combustion systems lies in the very  
53 high (>1500°C) operating temperatures. These high temperatures greatly limit material selection and  
54 require extensive combustor insulation. Further strong limitations of these devices are strictly related to  
55 their dimensions. As the size decreases, the surface area-to-volume ratio of the combustor increases with  
56 a subsequent increase of the heat-loss to heat-generation ratio. These strong losses in the small  
57 dimension induce flame quenching [1-3], and are also responsible for an increase in pollutants emission  
58 such as CO and unburned hydrocarbons. In addition, the smaller the volume, the shorter the flow  
59 residence time. To overcome such limitations, catalytic combustion seems to be the most suitable  
60 solution [31,32]. When implemented in micro/meso scale devices, catalytic combustion allows full  
61 utilization of the high energy densities of hydrocarbon fuels, but at notably lower operating temperatures  
62 than those typical of traditional combustion. Additionally, catalytic systems are generally easier to start,  
63 more robust to heat losses, and self-sustained at leaner fuel/air ratios [33-36].

64 When characterizing a catalytic combustor, catalyst degradation needs to be addressed [37]. The  
65 main mechanisms for platinum catalyst degradation include particle agglomeration, platinum loss and  
66 redistribution, and poisonous effects due to contaminants [38]. The catalyst degradation can be affected  
67 by the operating conditions, including temperature, humidity, and sources of contamination of catalyst  
68 active sites. Some studies concerning platinum aging show that no great effect on Pt catalyst is detected  
69 at automotive normal operating temperature (500°C), with consequently no substantial change in overall  
70 system performance [39]. Despite the huge amount of literature on catalyst degradation, no results for  
71 tests performed in conditions similar to those addressed in this work are available in literature.  
72 Therefore, in the present work, degradation tests were carried out on catalytic pellets.

73 In order to investigate the overall performance of a catalytic meso-scale combustor, the analysis of  
74 exhaust gases is required to derive chemical efficiency. Fourier transform infrared spectroscopy (FT-  
75 IR) has been widely applied for quantitative measurement of gas species concentrations of vehicles's  
76 exhaust [40,41]. Nevertheless, only a few works, such as [30], are reported in literature regarding the  
77 application of the FT-IR technique to measure gases concentration at the exhaust of a meso-scale  
78 combustor.

79 Compared to fuel cells or other combustion-based systems, thermoelectric (TE) power generators  
80 are attractive for portable systems due to their compactness, their reliability, their low energy  
81 consumption, and their high power densities. Considering commercial bismuth telluride-based TE  
82 modules, the operating temperature range is limited to 250°C, which is incompatible with the  
83 temperatures of a standard combustor. So, catalytic combustion is particularly well suited for TE power  
84 generation because of this relatively low temperature ceiling.

85 There are many examples of micro- and mesoscale thermoelectric power generators powered by  
86 catalytic combustion in available literature [42-46]. A TE generator fabricated from silicon bonded to  
87 glass developed by Yoshida et al. [46] was able to produce 184 mW of electrical power with an  
88 efficiency of 2.8% from the catalytic combustion of hydrogen. Norton and co-workers [5] reported for  
89 their integrated combustor-TE generator the production of 1W maximum power and a thermal-to-  
90 electrical conversion efficiency of 1.08% with hydrogen as the fuel. The group has also reported the  
91 generation of 0.45 W electrical power with propane as the fuel at 0.42% conversion efficiency, using  
92 propane lower heating value LHV [27]. In recent years, Marton and co-workers [47] developed a butane-  
93 fueled thermoelectric generator (TEG) delivering 5.82 W maximum power with 2.53% conversion  
94 efficiency. Several efforts have been made by different authors to investigate the hot gases recirculation  
95 in order to reduce heat losses and thus increase the efficiency of this kind of systems [48-50].  
96 Nevertheless, the demonstration of a fuel-based TEG suitable for portable power with energy density  
97 comparable to that of a battery remains an open challenge.

98 In this work, a new premixed catalytic combustor has been developed and characterized. The device  
99 has been designed for coupling with thermoelectric modules for portable electrical power production.  
100 The combustor is used as heat source in a sandwich between two TE modules, in order to achieve a  
101 larger electrical power output, with I-V characteristics suitable for supplying small electrical devices.  
102 Since the voltages obtained with small thermoelectric devices are usually too low for direct utilization,  
103 this feature is one of the most important advantages offered by the TEG presented in this work.

104 The meso-combustor developed in this work has notable advantages when compared to similar  
105 solutions presented in the literature [5-7]. The first advantage is the use of a low-cost, commercially

106 available catalyst, with no need for *ad hoc* manufacturing. The second important advantage is that the  
107 use of such a catalyst allows obtaining the desired wall temperatures for thermoelectric device coupling  
108 with no need for wall insulation from higher temperatures, thus resulting in smaller fuel consumption  
109 and a more compact design. The commercial TE modules chosen are not specifically designed for power  
110 applications, but the refined thermal control of the combustor allows producing up to 9.86 W of electrical  
111 power with a thermal to electrical conversion efficiency of 2.85%, resulting in an improvement in  
112 portable-scale electrical power converters based on thermoelectric technology and hydrocarbon fuels.

### 113 **Materials and Methods**

114 A thermoelectric generator was designed coupling a catalytic premixed meso-scale combustor and  
115 thermoelectric commercial modules. The sketch of the TEG developed is reported in Figure 1. Two TE  
116 modules are placed in a thermal chain consisting of the catalytic combustor surfaces (hot side) and two  
117 water-cooled heat sinks (cold side). In order to provide the most efficient contact at the interfaces  
118 between the TE modules with the combustor surface and the heat sink, graphite sheets (100  $\mu\text{m}$  thick)  
119 are used. Graphite was chosen for its capability for compensating the effects of surface roughness and  
120 was preferred to thermal pastes for its high reproducibility and stability. The heat sinks are aluminum  
121 bulks homogeneously cooled by a 13  $^{\circ}\text{C}$  water flowing in the circuit at 6 l/min volume rate. The cooling  
122 system is arranged in order to provide similar thermal conditions at both TEG sides. To ensure the  
123 thermal chain, the system is held together by two metal springs and four bolts and nuts. The compressive  
124 system allows obtaining a homogeneous pressure on the surfaces, minimizing thermal losses,  
125 compensating the increase of pressure on the TE modules due to the thermal expansion, and preserving  
126 the thermal chain components' correct alignment. In this work, 40 x 40  $\text{mm}^2$  Ferrotec commercial  
127 modules based on chalcogenides are used. These modules are designed for cooling applications, so no  
128 data specific for power generation are available. The operative limits below 260  $^{\circ}\text{C}$  considered in this  
129 work are derived considering the technologies used for thermoelectric elements soldering inside the  
130 device. Moreover, each module has been tested in order to define the conversion capability of the device,  
131 obtaining a response in terms of Seebeck effect of 30 mV/K and an internal resistance, useful for  
132 maximum power at the matching load calculation, of 3.94  $\Omega$ . The power output is a function both of the  
133 load and of the  $\Delta T$  applied to the module: using a  $\Delta T = 150$   $^{\circ}\text{C}$ , the maximum power produced by a  
134 single module is in the order of 3.8 W corresponding to a V-I couple of 3.5V and 1.1A, respectively.  
135

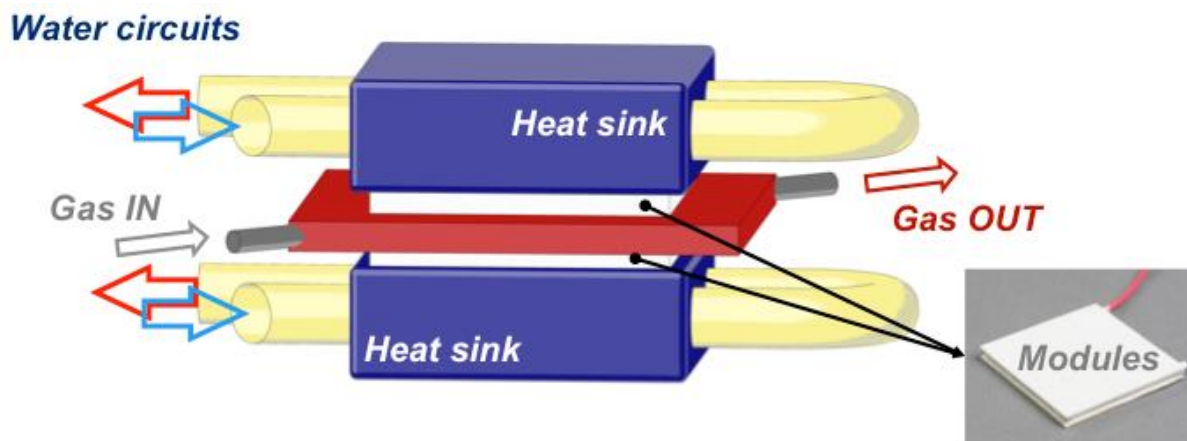


Figure 1. Sketch of the thermoelectrical generator obtained by coupling the combustor with two commercial thermoelectric modules.

136 The catalytic premixed meso-scale combustor was designed and characterized to be coupled to the  
137 TE modules [51]. The investigation was performed in order to assess the feasibility of the meso-scale  
138 combustor for the limits imposed by the modules used. Devices similar to the one presented in this work  
139 were proposed in [5], where the combustion channel is less than 1 mm high and the temperature at the  
140 combustor walls is too high for a direct coupling with thermoelectrics, thus requiring an intermediate  
141 cooling step. In the present work, the experimental conditions (e.g. combustion channel size, fuel/air

142 mass flow rates, etc) were chosen in order to reach the desired temperature without any cooling system  
143 at the interface between combustor and TE modules.

144 In Figure 2 a sketch of the combustor is shown. The geometry used for the combustion chamber  
145 was chosen in order to match the size of the TE devices. The aluminum-made combustor has a 40 x 40  
146 x 4 mm<sup>3</sup> chamber filled with 155 commercial alumina cylindrical pellets (r = 1.6 mm, h = 3.2 mm)  
147 covered with a thin catalytic film (platinum 1 % weight). The pellets are placed in ordered lines so that  
148 the height of the channel for gas flowing is 0.8 mm. Propane and air are used as fuel and oxidizer, and  
149 the related mass flow rates are measured and controlled by using thermal mass flow meters (Bronkhorst  
150 El-Flow F-201CV). As C<sub>3</sub>H<sub>8</sub>/air mixture is not self-igniting in contrast with H<sub>2</sub>/air mixture, hydrogen  
151 assisted ignition is performed.

152 The wall temperature distribution was measured with a Flir Systems ThermoVision A40 thermo  
153 camera using the values from K-type thermocouples placed on the combustor surface (A, B and C  
154 positions in Fig. 2) as absolute temperature reference for calibration. The accuracy in point  
155 measurements is about 0.5% ± 2°C in the temperature range considered (from -20°C to +350°C).

156 The overall chemical efficiency was estimated by means of Fourier transform infrared spectrometry  
157 (FT-IR) analysis of the exhaust gases. The exhaust gases were sent through a cut-off particulate filter  
158 and a water trap to a Thermo Scientific Nicolet 6700 FT-IR spectrometer equipped with a variable-  
159 pathlength heated gas-cell (Gemini Mars series 6.4M, internal volume of 0.75 l) positioned inside the  
160 instrument. In order to prevent possible carbon-residuals condensation, both the transfer line and the  
161 gas-cell were maintained at 393 K. To avoid exhaust gases dilution with ambient air, the suction mass  
162 flow was set to 6 NI/min to be lower than the outlet mass flow. The FT-IR spectra have a resolution of  
163 0.5 cm<sup>-1</sup>. The background was obtained with N<sub>2</sub> flow and subtracted from the spectra. Quantitative  
164 analyses of the gas concentrations were performed referring to a calibration based on mixtures of known  
165 compositions. The process chemical efficiency,  $\eta_c$ , was calculated using the relationship:

166 
$$\eta_c = \frac{[\text{CO}_2]}{[\text{CO}_2] + [\text{CO}] + [\text{UHC}]} \quad \text{Eq. (1)}$$

167 where [UHC] is the concentration of the total unburned hydrocarbons.  
168

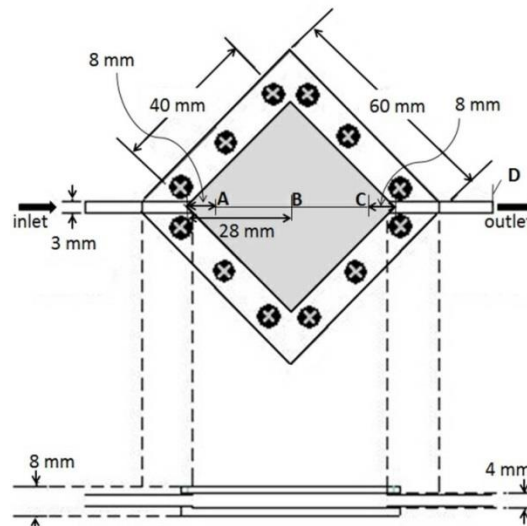


**Figure 2.** Sketch of the meso-scale combustor used in this work: the positions of the thermocouples used to measure the combustor wall temperature are indicate with A, B, C and D.

169 A peculiarity of thermoelectric technology is its long life with no need for maintenance. In order to  
170 consider the catalytic combustor a suitable heat source for the TEG, it was necessary to study the  
171 combustor components aging effects under operative conditions. In particular, attention was focused on  
172 the pellets used. An investigation of combustion processes effects on the degradation of the pellets  
173 catalytic coating was performed with metallographic analyses by using a scanning electron microscope  
174 (SEM) (FEG Hitachi SU-70) equipped with EDS and STEM detector.

175 The combustor was characterized at different operating conditions with the total mass flow rate  
 176 ranging between  $1.7 \times 10^{-5}$  and  $2.5 \times 10^{-5}$  kg/s varying the equivalence ratio,  $\Phi$ , in the range 0.8-1.2 by  
 177 changing both the propane and the air mass flow rate.

178 The TEG performance investigation was carried out at different operating conditions of the catalytic  
 179 combustor with the total mass flow rate ranging between  $6.3 \times 10^{-5}$  and  $14.6 \times 10^{-5}$  kg/s, keeping  $\Phi$  at  
 180 stoichiometric condition. Control of the final  $\Delta T$  applied to the TE modules was achieved varying the  
 181 inlet total mass flow rate, increasing in this way the hot side temperature. The cold side temperature  
 182 remained constant during the characterization process, due to the power removed by the water cooled  
 183 circuit, proving that the good thermal coupling of the TEG's different elements allowed obtaining a  
 184 good control of the stability at the cold side of the system. The TEG electrical output was studied in  
 185 terms of voltage and power produced for each  $\Delta T$  applied. The I-V and I-W characteristics were  
 186 measured at thermally steady conditions by connecting the TEG output to external loads having  
 187 increasing values from short-circuit up to open-circuit.

188 The data obtained from combustor and TEG characterization allowed calculating the electrical  
 189 conversion efficiency for each module and for the overall device.

### 190 Results and Discussion

191 The first step of the combustor characterization was assessing the total mass flow rate in order to  
 192 verify the temperature on the external walls at different conditions. Preliminary tests showed that the  
 193 lower combustion stability limit is at  $\Phi = 0.8$ , for  $2.5 \times 10^{-5}$  kg/s mass flow rate.

194 In Figure 3, the temperature values measured in the four positions versus  $\Phi$  for three different total  
 195 mass flow rates ( $1.7 \times 10^{-5}$  kg/s,  $2.1 \times 10^{-5}$  kg/s and  $2.5 \times 10^{-5}$  kg/s) are shown. The uncertainty in the  
 196 measured temperatures is approximately 6.67% in the worst case. Using  $50.35 \times 10^6$  J/kg for the propane  
 197 calorific value, thermal power values between 62 and 95 W were obtained for total mass flow rates  
 198 ranging from  $1.7 \times 10^{-5}$  kg/s to  $2.5 \times 10^{-5}$  kg/s, respectively.

199

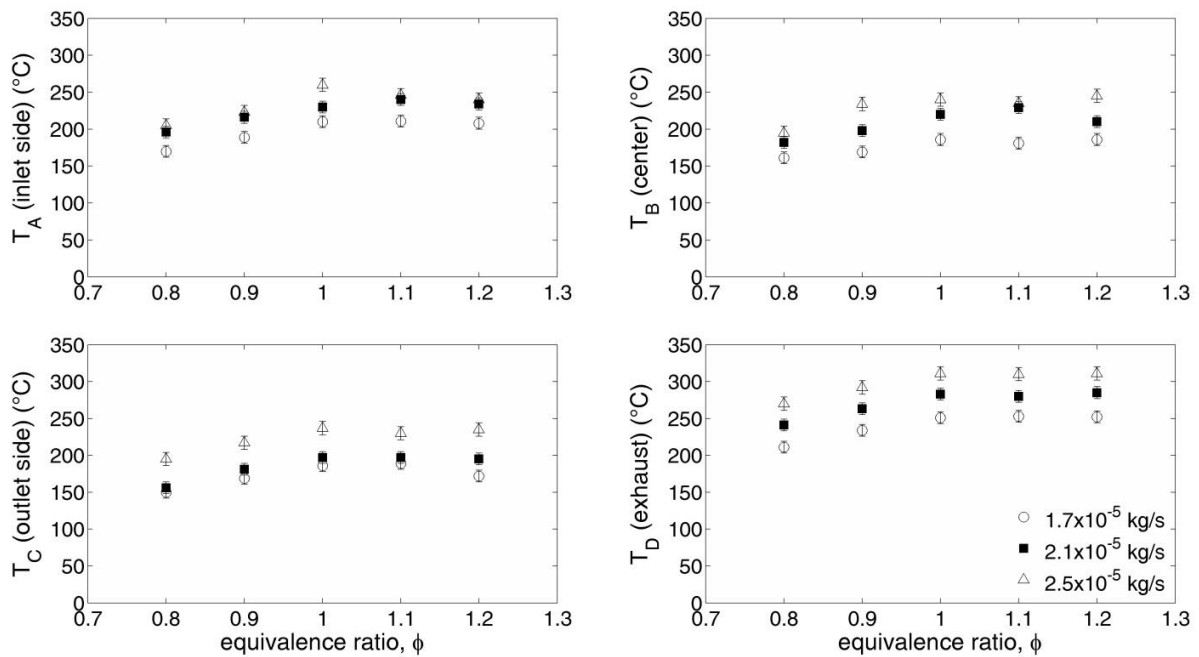


**Figure 3.** Temperature vs equivalence ratio at four different locations on the combustor wall and at three different mass flow rates.

200

201 As it can be noted, wall temperature increases with  $\Phi$  up to  $\Phi = 1$ , then remains approximately  
 202 constant for higher values. The behavior is similar for the three flow rates investigated at all positions.  
 203 The temperature slightly decreases moving downward from the inlet at fixed flow rate, and increases  
 204 monotonically with the flow rate. Exhaust gases temperature values are typically slightly above  $300^\circ\text{C}$ ,  
 205 which is higher than the walls temperatures in each condition.

206 The 2D temperature mapping on the combustor external walls is reported for different flow rates in  
 207 Figure 4. Only the actual combustion chamber surface has been considered. The arrows refer to the



208 mixture inlet and outlet. The actual inlet in the combustor is placed horizontally (45° rotation with  
 209 respect to the Figure).

210 The thermocamera images were calibrated using the thermocouple data previously described.  
 211 Investigation performed on both combustor sides showed no significant differences. The results prove  
 212 that the temperature on the external surface of the wall is satisfactorily uniform, thus confirming that the  
 213 meso combustor is a suitable hot source for the TEG. It can be noticed that the obtained temperature is  
 214 lower than the typical propane catalytic reaction temperature (700-800°C). This can be explained taking  
 215 into account the heat dissipation occurring at the combustor surface due to the thermal exchange with  
 216 ambient air. Considering the higher temperatures obtained at the combustor outlet (Figure 3), it is  
 217 reasonable to assume that the internal temperature matches the catalytic reaction temperature found in  
 218 literature.  
 219

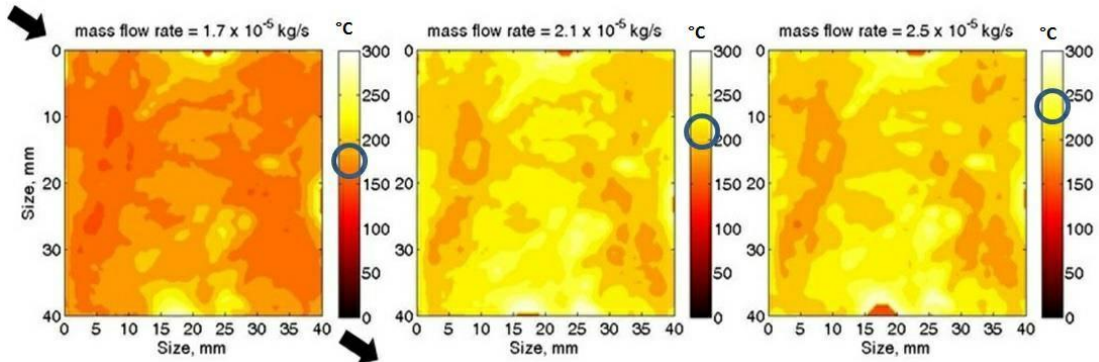


**Figure 4.** Temperature distribution on the combustor chamber external walls at three different mass flow rates. Arrows show gas inlet and outlet direction. Circles highlight the average temperature obtained in each case. Temperatures are given in Celsius degrees.

220  
 221 The FT-IR spectra of the gases collected at the exhaust of the premixed meso-scale combustor were  
 222 analyzed to determine their composition. After calibration, it was possible to perform quantitative  
 223 analyses with an estimated accuracy below 1% for FT-IR measurements.

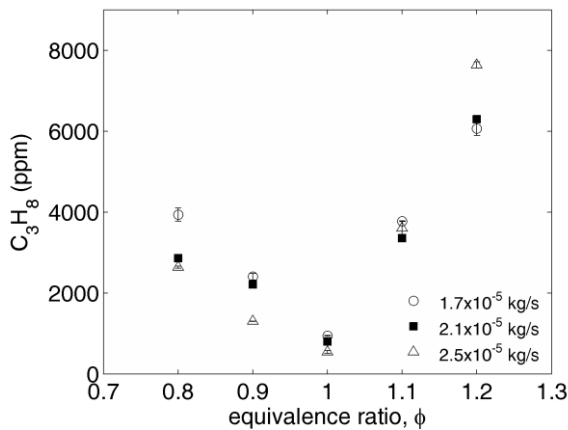


**Figure 5.** Combustor exhaust gases analysis: unburned propane concentration vs. equivalence ratio for three different mass flow rates.

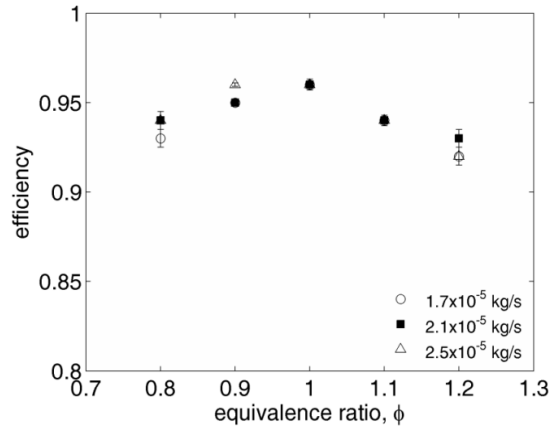


**Figure 6.** Chemical efficiency versus equivalence ratio for the mass flow rates investigated.

224  
 225 In Figure 5 propane concentration versus  $\Phi$  is reported for the three mass flow rates investigated.  
 226 In all cases, propane concentration profile shows a minimum at  $\Phi = 1$  as expected. For lower and higher  
 227 equivalence ratios, higher unburned propane was found at the combustor outlet. At  $\Phi = 1$ , the unburned  
 228 propane increases with the decrease of the mass flow rate, ranging from about 490 ppm for  $2.5 \times 10^{-5}$   
 229 kg/s mass flow rate to 940 ppm for  $1.7 \times 10^{-5}$  kg/s. The measurements error is small, with the uncertainty  
 230 in  $C_3H_8$  concentration being about 7.5% in the worst case.

231 CO<sub>2</sub> and CO concentrations were also measured. In both cases they increase with  $\Phi$ , reaching a  
232 plateau above  $\Phi = 1$ . The same behavior was obtained changing the mass flow rate values.

233 Taking into account the concentration measurements, it is possible to evaluate the chemical  
234 efficiency given by Eq. (1) where propane is the only unburned hydrocarbon detected. In Figure 6,  
235 efficiency vs. equivalence ratio is shown for all the tested flow rates. The uncertainty in the efficiency  
236 value is 0.5% in the worst case. A slight dependence on  $\Phi$  was observed, showing a maximum at the  
237 stoichiometric condition where about 96% efficiency is reached. For higher and lower  $\Phi$  values,  
238 efficiencies around 92-94% are obtained. Similar values of this chemical efficiency have been reported  
239 in literature [5], referring to a different combustor fueled with the same mixture at higher flow rates.

240 The results reported for the catalytic combustor characterization prove that the system thermal  
241 control and homogeneity are suitable for coupling the combustor with TE modules obtaining good  
242 chemical efficiency.

243 As complementary analyses to evaluate the combustor life span, tests on pellet degradation were  
244 performed. The pellets underwent 200 h operating combustion conditions, and the evolution of the active  
245 phase was verified with SEM analyses. It is reasonable to expect that the degradation takes place at  
246 typical temperature values of catalytic combustion (e.g. 700-800 °C) [35]. In these conditions, coking,  
247 agglomeration and contamination effects of the catalytic pellets are likely to occur, which could affect  
248 the performance of the overall system.

249 SEM images (backscattered electrons) for fresh and used (200 h) pellets surfaces are shown in  
250 Figure 7. It can be noted that used pellets show white agglomerates spread over the surface which do  
251 not appear on the fresh pellets surface. EDX analyses suggest that these agglomerates consist of  
252 Platinum, while the main material is almost entirely alumina.

253

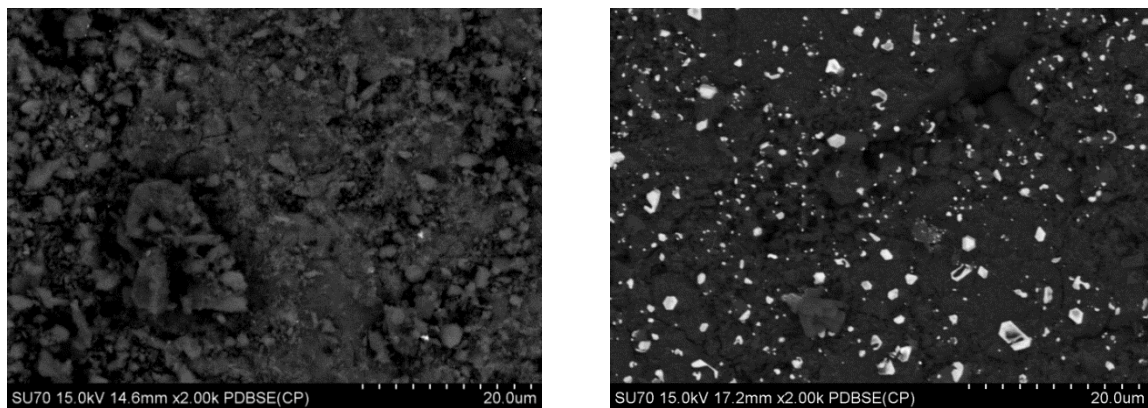


**Figure 7.** SEM backscattered micrographs of fresh (left) and 200 h aged (right) pellet base surface.

254

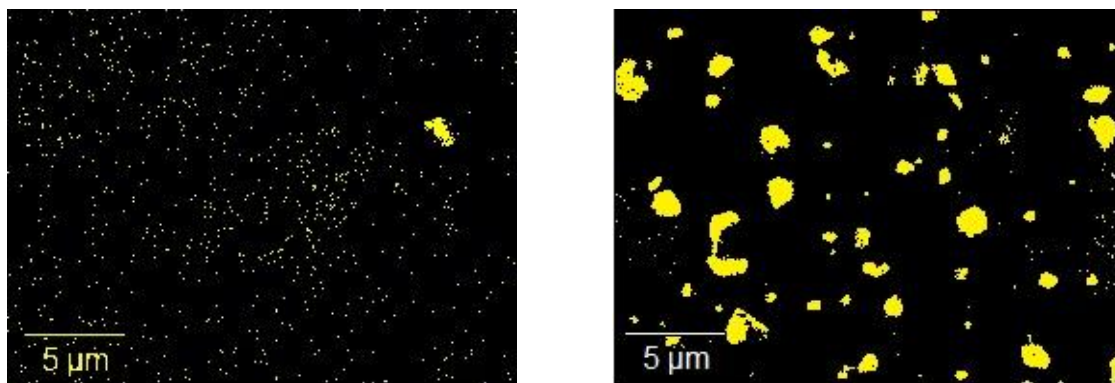


**Figure 8.** EDX mapping of Pt distribution on fresh (left) and 200 h aged (right) pellets surface.

255

256 Pt distribution mapping of the pellets' surface (Figure 8) highlights that very small Pt spots are  
257 spread on the fresh pellets' surface, while the used pellets' surface shows fewer but much larger Pt  
258 structures reaching a size of 2-3  $\mu\text{m}^2$ . Thus, the pellets morphology evolves in operating time due to the

259 combustion temperature and the catalyzer aggregates forming particles which could affect its efficiency  
 260 in supporting the combustion. However, after 200 h the combustor performances seemed not to be  
 261 affected by this evolution and the combustor maintains its characteristics.

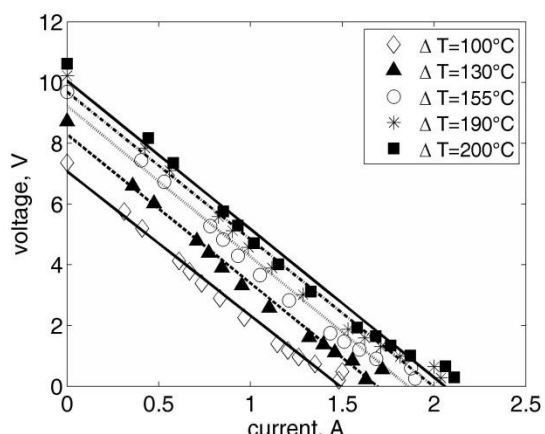


Figure 9. Power delivered by the TEG vs. current.

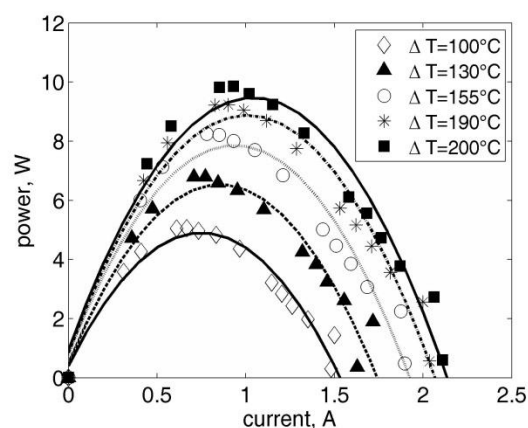


Figure 10. Voltage of TEG vs. current.

262  
 263 In Figures 9 and 10, the results of the characterization of the coupled system, catalytic combustor  
 264 and TE modules, in terms of electrical output of the TEG are reported. The output voltage (V) and the  
 265 electrical power (W), respectively, are plotted as a function of the current produced for different  $\Delta T$   
 266 applied. The maximum power delivered by the device ranges between 5 and 10 W for  $\Delta T$  values ranging  
 267 between 100 and 200°C. Correspondingly, the voltage drop across the load is in the range 7.5 – 10 V.  
 268 The values obtained are consistent with the preliminary characterization at different thermal conditions  
 269 performed on the commercial modules used.

270 The experiments on the TEG were performed for different total (propane + air mixture) mass flow  
 271 rates resulting in different  $\Delta T$  between the hot and cold sides. Experimental parameters for the different  
 272 tests and the results obtained are summarized in in Table 1. Each total mass flow rate condition was  
 273 obtained keeping  $\Phi$  constant at stoichiometric conditions and by varying the propane and air mass flow  
 274 rates.

275  
 276 **Table 1.** Maximum TE power obtained, power provided, and conversion efficiency at different  
 277 mass flow rate and  $\Delta T$  values.

mixture mass flow rate Kg/s	$\Delta T$ °C	$T_{hot}$ °C	power provided W	power obtained W	conversion efficiency %
$6.3 \times 10^{-5}$	100	179	178.71	5.06	2.83
$8.4 \times 10^{-5}$	130	207	238.29	6.78	2.85
$10.3 \times 10^{-5}$	155	233	297.86	8.24	2.77
$12.6 \times 10^{-5}$	190	245	357.43	9.24	2.59
$14.6 \times 10^{-5}$	200	258	417.00	9.86	2.36

278  
 279 It can be noted that all the mass flow rate conditions used for TEG characterization are higher than  
 280 those previously reported for the combustor alone. This is because when the combustor is coupled with  
 281 the TE modules and the cooling system, the desired temperature at the combustor surface (up to 250°C  
 282 at the hot side) is obtained for higher flow rates due to the increased thermal exchange. The minimum  
 283 mass flow rate ( $6.3 \times 10^{-5}$  kg/s) corresponds to the limit under which the combustion is no longer  
 284 sustained, while the maximum mass flow rate ( $14.6 \times 10^{-5}$  kg/s) is the limit over which no further  $\Delta T$   
 285 increase is obtained with the cooling system used.



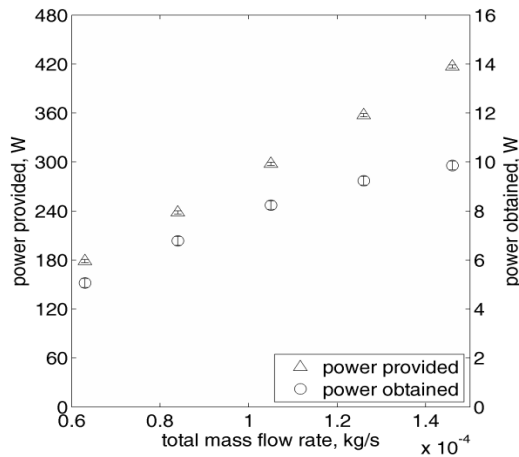


**Figure 11.** Power provided to the TEG (based on LHV) and power obtained vs. mixture mass flow rate.

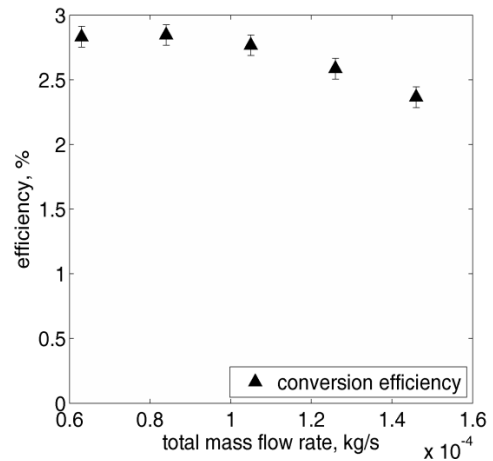


**Figure 12.** Efficiency of thermal to electric power conversion vs. mixture mass flow rate.

286

287

288

289

290

291

292

293

294

295

296

297

298

299

300

301

302

303

304

305

306

307

308

309

The power provided to and the power delivered from the device are plotted in Figure 11 as a function of total mass flow rate. It can be noted that the obtained power curve slope tends to decrease for higher mass flow rates, indicating that the system is approaching its maximum performance at the given cooling conditions. No higher mass flow rate was tested in this work because at  $14.6 \times 10^{-5}$  a combustor surface temperature of  $255^{\circ}\text{C}$  was reached, which is the maximum allowed for the TE modules used. The uncertainty on the experimental point is  $\pm 2$  W for the power provided to the system and  $\pm 0.8$  for the power obtained.

In order to obtain the device thermal to electrical conversion efficiency, the power provided to the system was calculated as the propane mass delivered in each testing case times its lower heating value (LHV). Figure 12 shows the thermal to electrical conversion efficiency obtained for the different mass flow rate values tested. The maximum efficiency obtained is around 2.85%. Similar values are obtained for mass flow rates values up to  $10.3 \times 10^{-5}$  kg/s, while for higher mass flow rates the efficiency tends to decrease. This behavior can be explained considering the effect of increased mass flow rate on exhaust concentration described before: unburnt propane concentration increases with increasing mass flow rates due to the reduced residence time. This leads to a lower propane conversion efficiency which negatively affects the thermal to electrical conversion.

A comparison with similar devices described in literature is shown in Table 2, in which the overall power produced and the thermal to electrical conversion efficiency in different TEGs based on catalytic combustion are shown. The TEG presented in this work represents an improvement in the conversion efficiency compared to other published works.

**Table 2.** Comparison of the TE power generation obtained in this work with those of other published works.

source	fuel	overall power produced, W	conversion efficiency %
<b>Federici, 2006</b> <sup>[27]</sup>	propane	0.45	0.42
<b>Norton, 2004</b> <sup>[5]</sup>	hydrogen	1	1.08
<b>Marton, 2011</b> <sup>[47]</sup>	butane	5.82	2.53
<b>Yoshida, 2006</b> <sup>[46]</sup>	hydrogen	0.18	2.8
<b>This work</b>	propane	9.86	2.85

310

311

312

313

314

Future developments of the TEG device presented in this work will include an upgrade of the ignition system with inlet gases preheated through exhaust gases recycling, and preheated inlet gases replacing the hydrogen-assisted ignition.

## 315 **Concluding Remarks**

316 A novel premixed catalytic meso-scale combustor fueled with propane/air was developed to be coupled  
317 with a thermo-electric device for portable electric applications. Due to the need to use commercially-  
318 available thermoelectric devices, the limitation of temperature at 250°C was a stringent requirement to  
319 match. Therefore, the proper mass flow rate value was found inside the stability limits which produced  
320 reasonable values of temperature on the combustor surfaces. In order to investigate the temperature  
321 distribution on the combustor surfaces, temperature measurements were carried out by using an IR  
322 camera. A uniform distribution on both sides was obtained, assuring thermo-electric conversion  
323 optimization.

324 Quantitative analysis of the gas-species concentration of the exhaust was performed by FT-IR  
325 measurements. From these measurements, the propane conversion efficiency values were derived in the  
326 different experimental conditions under study. It was found that reasonable high efficiency of about  
327 96% was obtained at the stoichiometric condition.

328 Considering the catalytic pellets degradation during combustion, a change of the distribution of Pt  
329 on the alumina surface was observed, resulting in bigger and more complex structures. No significant  
330 effects of the coating degradation on the overall combustor performance were observed after 200 h.  
331 These results suggest that the combustor proposed is suitable for thermo-electric conversion application.  
332 The controlled combustion conditions and the low consumption of the Pt layer suggest a longer expected  
333 lifetime for a catalytic combustor in comparison to a traditional combustor. This aspect couples the  
334 thermoelectric device advantage in terms of long life without maintenance: the generator has no moving  
335 parts and demonstrates long-lasting operative stability.

336 The catalytic combustor was integrated with TE modules to produce 9.86 W of electrical power  
337 with a thermal to electrical conversion efficiency of 2.85%. The proposed device represents a notable  
338 improvement in portable-scale electrical power production from hydrocarbon fuels, with an increase in  
339 the conversion efficiency compared to other published works.

340 Future perspectives include reducing the system scale, and exploiting the hot gases recirculation in  
341 order to reduce the heat losses and further increase the thermal to electrical conversion efficiency. The  
342 downscale of the dimension is going to focus on maintaining the highest possible level of power  
343 production but with a specific care for the voltage level obtained, in order to ensure both ranges are  
344 suitable for power supplying of portable electronic devices.  
345

## 346 **Acknowledgements**

347 The authors would like to acknowledge the financial support for the project INTEGRATE in the  
348 framework of CNR-Regione Lombardia program, the technical assistance of Mr Fantin, and Ms. Paula  
349 Albin Reynolds for editing contribution.

350

## 351 **References**

352 [1] Vican, J. G. B. F., Gajdeczko, B. F., Dryer, F. L., Milius, D. L., Aksay, I. A., and Yetter, R. A.,  
353 "Development of a microreactor as a thermal source for microelectromechanical systems power  
354 generation", *Proceedings of the Combustion Institute*, 29(1): 909-916 (2002).

355 [2] Maruta, K., "Micro and mesoscale combustion", *Proceedings of the Combustion Institute*, 33(1), 125-150  
356 (2011).

357 [3] Yang, W. M., Chou, S. K., Shu, C., Xue, H., Li, Z. W., Li, D. T., and Pan, J. F., "Microscale combustion  
358 research for application to micro thermophotovoltaic systems", *Energy Conversion and Management*, 44(16),  
359 2625-2634 (2003).

360 [4] Fernandez-Pello, A.C., "Micropower Generation Using Combustion: Issues and Approaches",  
361 *Proceedings of the Combustion Institute*, 29: 883-899 (2002).

362 [5] Norton, D. G., Voit, K. W., Brüggemann, T., Vlachos, D. G., and Wetzel, E. D. "Portable power  
363 generation via integrated catalytic microcombustion-thermoelectric devices", in *24th Army Science Conference*,  
364 *Orlando, FL*, 2004.

365 [6] Hua, J., Wu, M., and Kumar, K., "Numerical simulation of the combustion of hydrogen-air mixture in  
366 micro-scaled chambers Part II: CFD analysis for a micro-combustor", *Chemical engineering science*, 60(13),  
367 3507-3515 (2005). Patil, A. S., Dubois, T. G., Sifer, N., Bostic, E., Gardner, K., Quah, M., & Bolton, C., "Portable  
368 fuel cell systems for America's army: technology transition to the field", *Journal of Power Sources*, 136(2), 220-  
369 225 (2004).

370 [7] Yadav, S., Sharma, P., Yamasani, P., Minaev, S., and Kumar, S., "A prototype micro-thermoelectric  
371 power generator for micro-electromechanical systems", *Applied Physics Letters*, 104(12), 123903 (2014).

372 [8] Dunn-Rankin, D., Leal, E.M., Walther, D.C., "Personal power systems", *Progress in Energy and*  
373 *Combustion Science* 31: 422–465 (2005).

374 [9] Choi, W., Kwon, S., and Dong Shin, H., "Combustion characteristics of hydrogen–air premixed gas in a  
375 sub-millimeter scale catalytic combustor", *International Journal of Hydrogen Energy*, 33(9), 2400-2408 (2008).

376 [10] Norton, D.G., Wetzel, E.D., and Vlachos, D.G., "Fabrication of single-channel catalytic microburners:  
377 effect of confinement on the oxidation of hydrogen/air mixtures", *Industrial & Engineering Chemistry Research*  
378 43, 4833–4840 (2004).

379 [11] Wierzbicki, T. A., Lee, I. C., and Gupta, A. K. "Combustion of propane with Pt and Rh catalysts in a  
380 meso-scale heat recirculating combustor", *Applied Energy*, 130, 350-356 (2014).

381 [12] Pattekar, A.V., Kothare, M.V., "A radial microfluidic fuel processor", *Journal of Power Sources* 147:  
382 116–127 (2005).

383 [13] Norton, D.G., and Vlachos, D.G., "A CFD study of propane/air microflame stability". *Combustion and*  
384 *Flame* 138, 97–107 (2004).

385 [14] Kaisare, N.S., Vlachos, D.G., "Optimal reactor dimensions for homogeneous combustion in small  
386 channels", *Catalysis Today* 120: 96–106 (2007).

387 [15] Miesse, C. M., Masel, R. I., Jensen, C. D., Shannon, M. A., and Short, M., "Submillimeter-scale  
388 combustion". *AIChE Journal*, 50 12: 3206-3214 (2004).

389 [16] Kaisare, N.S., Deshmukh, S.R., and Vlachos, D.G., "Stability and performance of catalytic  
390 microreactors: Simulations of propane catalytic combustion on Pt", *Chemical Engineering Science* 63, 1098-1116  
391 (2008).

392 [17] Norton, D.G., Wetzel, E.D., and Vlachos, D.G., "Thermal management in catalytic microreactors",  
393 *Industrial & Engineering Chemistry Research* 45: 76–84 (2006).

394 [18] Ouyang, X., Bednarova, L., Besser, R. S., and Ho, P., "Preferential oxidation (PrOx) in a thin-film  
395 catalytic microreactor: Advantages and limitations", *AIChE journal*, 51(6), 1758-1772 (2005).

396 [19] Rebrov, E. V., De Croon, M. H. J. M., and Schouten, J. C., "A kinetic study of ammonia oxidation on a  
397 Pt catalyst in the explosive region in a microstructured reactor/heat-exchanger", *Chemical Engineering Research*  
398 *and Design*, 81(7), 744-752 (2003).

399 [20] Deshmukh, S.R., and Vlachos, D.G., "A reduced mechanism for one-step rate expressions for catalytic  
400 combustion of small alkanes on noble metals", *Combustion and Flame* 149: 366–383 (2007).

401 [21] Saracco, G., Veldsink, J. W., Versteeg, G. F., and van Swaaij, W. P., "Catalytic combustion of propane  
402 in a membrane reactor with separate feed of reactants—II. Operation in presence of trans-membrane pressure  
403 gradients", *Chemical engineering science*, 50(17), 2833-2841 (1995).

404 [22] Deshmukh, S. R., Mhadeshwar, A. B., Lebedeva, M. I., and Vlachos, D. G. "From density functional  
405 theory to microchemical device homogenization: model prediction of hydrogen production for portable fuel cells",  
406 *International Journal for Multiscale Computational Engineering*, 2(2) (2004).

407 [23] Ganley, J. C., Seebauer, E. G., and Masel, R. I., "Development of a microreactor for the production of  
408 hydrogen from ammonia", *Journal of Power Sources*, 137(1), 53-61 (2004).

409 [24] Deshmukh, S. R., and Vlachos, D. G. "Effect of flow configuration on the operation of coupled  
410 combustor/reformer microdevices for hydrogen production", *Chemical Engineering Science*, 60(21), 5718-5728  
411 (2005).

412 [25] Kolios, G., Glöckler, B., Gritsch, A., Morillo, A., and Eigenberger, G., "Heat-Integrated Reactor Concepts  
413 for Hydrogen Production by Methane Steam Reforming", *Fuel Cells*, 5(1), 52-65 (2005).

414 [26] Norton, D., Deshmukh, S. R., Wetzel, E. D., and Vlachos, D. G., "Downsizing chemical processes for  
415 portable hydrogen production", *ACS symposium series* (Vol. 914, pp. 179-193). Oxford University Press (2005).

416 [27] Federici, J. A, Norton, D. G., Bruggeman, T., and Voit, K.W., "Catalytic Microcombustor with integrated  
417 thermoelectric element for portable production", *Journal of Power Sources* 161, 1469-1478 (2006).

418 [28] Ahn, J., Eastwood, C., Sitzki, L., and Ronney, P. D., "Gas-phase and catalytic combustion in heat-  
419 recirculating burners", *Proceedings of the Combustion Institute*, 30(2), 2463-2472 (2005).

420 [29] Zhang, S., Yuan, X. Z., Hin, J. N. C., Wang, H., Friedrich, K. A., and Schulze, M., "A review of platinum-  
421 based catalyst layer degradation in proton exchange membrane fuel cells", *Journal of Power Sources* 194.2 (2009):  
422 588-600.

423 [30] Wu, M., Yetter, R.A., and Yang, V., "Combustion in meso-scale vortex combustors: experimental  
424 characterization", 42nd AIAA Aerospace Sciences Meeting and Exhibit, 5-8 Jan. 2004, Reno, Nevada. AIAA  
425 2004-980 (2004).

426 [31] Wierzbicki, T.A., Lee, I.C., and Gupta, A.K.. "Combustion of propane with Pt and Rh catalysts in a meso-  
427 scale heat recirculating combustor." *Applied Energy* 130 (2014): 350-356.

428 [32] Neyestanaki, A. K., Kumar, N., and Lindfors, L-E. "Catalytic combustion of propane and natural gas over  
429 Cu and Pd modified ZSM zeolite catalysts." *Applied Catalysis B: Environmental* 7.1 (1995): 95-111.

430 [33] Vijayan, V., and Gupta, A.K., "Combustion and Heat Transfer at Meso-scale with thermal recuperation",  
431 *J. Applied Energy*, Vol. 87, No. 8, August 2010, pp. 2628-2639.

432 [34] Vijayan, V., and Gupta, A.K., "Flame Dynamics of a Meso-scale Heat Recirculating Combustor", *J.*  
433 *Applied Energy*, Vol. 87, No. 12, December 2010, pp. 3718-3728.

434 [35] Vijayan, V., and Gupta, A.K., "Thermal Performance of a Meso scale Liquid Fuel Combustor", *J. Applied*  
435 *Energy*, Vol. 88, issue 7, 2011, pp. 2335-2343.

436 [36] Shirsat, V, and Gupta, A.K., "Performance Characteristics of Methanol and Kerosene Fuelled Meso-  
437 Scale Heat Recirculating Combustors", *J. Applied Energy*, Volume 88, 2011, pp. 5069-5082.

438 [37] Yazawa, Y., Takagi, N., Yoshida, H., Komai, S. I., Satsuma, A., Tanaka, T., Yoshida, S., and Hattori, T.,  
439 "The support effect on propane combustion over platinum catalyst: control of the oxidation-resistance of platinum  
440 by the acid strength of support materials." *Applied Catalysis A: General* 233.1 (2002): 103-112.

441 [38] González-Velasco, J. R., Botas, J. A., Ferret, R., Pilar González-Marcos, M., Marc, J. L., and Gutiérrez-  
442 Ortiz, M. A., "Thermal aging of Pd/Pt/Rh automotive catalysts under a cycled oxidizing-reducing  
443 environment", *Catalysis today* 59.3 (2000): 395-402.

444 [39] Mayrhofer, K. J., Meier, J. C., Ashton, S. J., Wiberg, G. K., Kraus, F., Hanzlik, M., and Arenz, M., "Fuel  
445 cell catalyst degradation on the nanoscale", *Electrochemistry Communications* 10.8 (2008): 1144-1147.

446 [40] Hanst, P. L., "Infrared spectroscopy and infrared lasers in air pollution research and monitoring", *Applied*  
447 *Spectroscopy*, 24(2), 161-174 (1970).

448 [41] Baum, M. M., Kiyomiya, E. S., Kumar, S., Lappas, A. M., Kapinus, V. A., and Lord, H. C.,  
449 "Multicomponent remote sensing of vehicle exhaust by dispersive absorption spectroscopy. 2. Direct on-road  
450 ammonia measurements", *Environmental science & technology*, 35(18), 3735-3741 (2001).

451 [42] Aranguren, P., Astrain, D., Rodríguez, A., and Martínez, A. "Experimental investigation of the  
452 applicability of a thermoelectric generator to recover waste heat from a combustion chamber." *Applied Energy* 152  
453 (2015): 121-130.

454 [43] Chou, S. K., Yang, W.M., Chua, K.J., Li, J., and Zhang, K.L. "Development of micro power  
455 generators—a review." *Applied Energy* 88.1 (2011): 1-16.

456 [44] Kinsella, C. E., O'Shaughnessy, S.M., Deasy, M.J., Duffy, M., and Robinson, A.J. "Battery charging  
457 considerations in small scale electricity generation from a thermoelectric module." *Applied Energy* 114 (2014):  
458 80-90.

459 [45] Xiao, H., Qiu, K., Gou, X., and Ou, Q. "A flameless catalytic combustion-based thermoelectric generator  
460 for powering electronic instruments on gas pipelines." *Applied Energy* 112 (2013): 1161-1165.

461 [46] Yoshida, K., Tanaka, S., Tomonari, S., Satoh, D., and Esashi, M., "High-energy density miniature  
462 thermoelectric generator using catalytic combustion". *Microelectromechanical Systems, Journal of*, 15(1), 195-  
463 203 (2006).

464 [47] Marton, C.H., Haldeman, G.S., and Jensen, K.F., "Portable thermoelectric power generator based on a  
465 microfabricated silicon combustor with low resistance to flow". *Industrial & Engineering Chemistry*  
466 *Research*, 50(14), 8468-8475 (2011).

467 [48] Shirsat, V., and A. K. Gupta. "A review of progress in heat recirculating meso-scale combustors." *Applied*  
468 *Energy* 88.12 (2011): 4294-4309.

469 [49] Tolmachoff, Erik D., William Allmon, and C. Mike Waits. "Analysis of a high throughput n-dodecane  
470 fueled heterogeneous/homogeneous parallel plate microreactor for portable power conversion." *Applied*  
471 *Energy* 128 (2014): 111-118.

472 [50] Vijayan, V., and A. K. Gupta. "Combustion and heat transfer at meso-scale with thermal  
473 recuperation." *Applied Energy* 87.8 (2010): 2628-2639.

474 [51] Merotto, L., Dondè, R., and De Iuliis, S., "Study of the Performance of a Catalytic Premixed Meso-scale  
475 Burner", Ninth Mediterranean Combustion Symposium, Rhodes, Greece, 7-11 June 2015.